JOURNAL OF FORENSIC SCIENCES

J Forensic Sci, January 2010, Vol. 55, No. 1
doi: 10.1111/j.1556-4029.2009.01217.x
Available online at: interscience.wiley.com

PAPER

CRIMINALISTICS

Alex J. Goddard,[1] *M.Chem.; A. Robert Hillman,*[1] *D.Phil.; and John W. Bond,*[2] *D.Phil.*

High Resolution Imaging of Latent Fingerprints by Localized Corrosion on Brass Surfaces

ABSTRACT: The Atomic Force Microscope (AFM) is capable of imaging fingerprint ridges on polished brass substrates at an unprecedented level of detail. While exposure to elevated humidity at ambient or slightly raised temperatures does not change the image appreciably, subsequent brief heating in a flame results in complete loss of the sweat deposit and the appearance of pits and trenches. Localized elemental analysis (using EDAX, coupled with SEM imaging) shows the presence of the constituents of salt in the initial deposits. Together with water and atmospheric oxygen—and with thermal enhancement—these are capable of driving a surface corrosion process. This process is sufficiently localized that it has the potential to generate a durable negative topographical image of the fingerprint. AFM examination of surface regions *between* ridges revealed small deposits (probably microscopic "spatter" of sweat components or transferred particulates) that may ultimately limit the level of ridge detail analysis.

KEYWORDS: forensic science, latent fingerprint, atomic force microscope, imaging, localized corrosion, metal surface

A recent publication (1) demonstrated the feasibility of acquiring fingerprints on metallic surfaces subject to heat, as might be experienced by objects in a fire or by a bullet in a firearm. It would appear that exposure to high temperatures—sufficient to destroy more fragile forensic evidence—is in fact central to the creation of an indelible image in the metal surface. The suggestion was that the image is formed by a localized corrosion-like process that leaves an etching of the ridge detail in the metal. This phenomenon has considerable potential application in a wide variety of criminal investigations, but will only become a reliable method if it is possible to determine the nature of the processes involved, the types of metal surface on which it can occur, and the conditions that optimize the development of the image. This study sets out to address the first of these questions—the answers to which should be the prerequisites for addressing the remaining issues—for the specific case of brass substrates, which are relevant to a range of items, notably bullet casings. This is accomplished using a high resolution imaging device, the Atomic Force Microscope (AFM), which has found wide applicability in characterizing diverse metallic (2), polymer (3), and organic (4) surfaces and is now widely exploited in interfacial science (5–7).

Background

Although the ability of latent fingerprint deposits to undergo a chemical reaction with metal substrates has been known for many years (8), it is only recently that this reaction has been exploited to develop techniques to visualize fingerprint ridges. One advantage of these techniques is that they are noninvasive, that is, no physical or chemical development of the fingerprint is required prior to visualization unlike conventional treatments such as powdering, cyanoacrylate fuming, suspension in small particle reagents (9–11), or electrochemical etching (12–15). Therefore, such techniques offer the potential to visualize the fingerprint after the deposit has been removed from the metal by, for example, washing or rubbing. This has practical relevance to damage accruing to items prior to evidence collection or as a result of poor handling thereafter.

Williams et al. (16,17) have demonstrated fingerprint visualization on a variety of metal surfaces using a Scanning Kelvin Microprobe. This technique is based on a measurement of the potential difference arising between a wire probe and the metal surface due to differences in their respective work functions, the magnitude of this potential difference being affected by the fingerprint deposit. By measuring this variation in magnitude, an image of the fingerprint has been visualized in terms of potential difference. The usefulness of this technique was demonstrated by visualizing fingerprints deposited beneath layers of soot or paint and also on brass cartridge cases where fingerprints were deposited postfiring.

More recently, one of us considered the effect that fingerprint deposits had on a range of metal elements and alloys (1,18). Heating the metal to several hundred degrees Celsius produced durable images of fingerprints that enabled fingerprint visualization even after the metal had been subject to smoke and soot contamination or spray painting. Similarly durable images were found to occur by leaving fingerprint deposits on metal in air at room temperature for several days. When the metal substrate consisted of brass, further work revealed that the junction between the brass and fingerprint image could exhibit the characteristics of a rectifying metal-semiconductor contact with the composition of the fingerprint image exhibiting the properties of a p-type semiconductor (19). This type of rectifying metal-semiconductor contact is commonly known as a Schottky barrier (20–22).

Consistent with generally accepted fact in the field of corrosion science, Williams et al. (16,17) and Bond (1,19) considered the degree of visualization of fingerprint deposits left in air at room

[1]Department of Chemistry, University of Leicester, Leicester LE1 7RH, U.K.
[2]Scientific Support Department, Northamptonshire Police, Wootton Hall, Northampton NN4 0JQ, U.K. Also at: Forensic Research Centre, University of Leicester, Leicester LE1 7RH, U.K.

Received 31 Oct. 2008; and in revised form 19 Dec. 2008; accepted 1 Jan. 2009.

temperature to be associated with the presence of ionic salts in the deposit. The salt solution (formed from the salt and water in the deposit) acts as the electrolyte in an electrochemical reaction between the deposit and the metal, resulting in corrosion to the metal surface. Further, Bond postulated that variations in the degree of visualization of fingerprint deposits between individuals was due to both the variable composition of sweat and the amount of sweat secreted by different individuals (18).

Objectives

The generation of an etched image of a fingerprint on a metal surface has unequivocally been demonstrated (1) but the underlying physical and chemical processes that generate the image are unknown. The generic objective of this work is to determine the nature of these processes. Specific goals that follow from this are identification of the key chemical species, conditions that enhance (or inhibit) image generation and, via these, the types of metal surface likely to be susceptible to etching in this manner.

Novelty and Significance

Whilst prior work has demonstrated the ability of fingerprint deposits to produce durable images through corrosion of metal, the authors can find no research that has attempted to visualize corrosion of the metal surface at the nanometer scale. Such work is of value in order to provide a better understanding of the mechanism for the reaction between the fingerprint deposit and the metal and also the effects that the reaction has on the surface of the metal. In this paper, we show how an AFM may be used to visualize the reaction products on brass substrates subjected to a variety of environmental conditions after deposition of a fingerprint. We consider the results obtained in terms of the corrosion mechanism described above and also indicate the direction for future work in this area.

Materials and Methods

Imaging Methodology

The dimensions of whole fingerprints (on the order of a centimeter) and individual ridges (on the order of hundreds of micrometers) mean that they can readily be viewed directly or with the aid of simple optical magnifying devices. However, since the goal of the present study is to elucidate the origins and nature of highly localized corrosion associated with fingerprint residue on metallic surfaces, the requirement is a means of imaging at much higher resolution, typically 1 μm or less. The technique selected for this purpose is the AFM (5–7), which has been shown to be capable of providing topographic images of a wide range of surfaces with vertical and lateral resolutions of <10 nm. For the instrument used in the present study (see below), this capability was exploited within a typical lateral footprint (total image size) of 100 μm × 100 μm, and a maximum travel (vertical range) of 9 μm.

The AFM technique involves holding a finely etched tip (typical radius of curvature 10 nm; Veeco model RTESP part # MPP-11100-10; operating frequency 250–350 kHz and spring constant 20–80 N m^{-1}, dependent on conditions) mounted on a sensitive cantilever in close proximity to the surface of the sample and measuring the interaction force between the tip and sample surface as a function of lateral position. The distance between the sample surface and the tip is uniquely defined by the interaction force, which is measured optically and converted into a topographic map (5–7). Since this interaction is not determined by sample conductivity, the AFM will image both exposed metal areas of the sample and areas coated with fingerprint residue. The latter (which are likely to be electrically insulating) could not be imaged by the closely related Scanning Tunnelling Microscope (STM) (23–25), which relies on passage of electrical current between the tip and sample surface.

The instrument used was a Veeco Dimension 3100 Scanning Probe Microscope (Veeco, Santa Barbara, CA), operated via Nanoscope version 6.12r1 software (Veeco). The tips were phosphorus-(n-) doped silicon, with a nominal radius of 10 nm and their operation was calibrated using silicon wafer standards. Dependent on whether the tip is very close to, or somewhat further from, the sample the force may be repulsive or attractive in nature. This gives rise to three modes of operation—so-called contact, noncontact, and tapping modes—each of which has characteristics suited to particular types of sample. In contact mode, there is a danger that soft material (such as the fingerprint residue) may be deformed, rather than imaged, by the much harder tip; this mode was therefore not selected. In noncontact mode, there is the possibility for surfaces with strongly varying surface contours that the tip may ''crash'' into raised parts of the sample. In the present case, the system was operated in tapping mode, in which the tip is oscillated (''tapped'') above the surface, in such a manner as to avoid physical deformation of the mechanically soft components of the sample. An optical microscope attached to the AFM was used to survey the surface at low resolution and to identify individual features for higher resolution imaging using the AFM tip; the optical image could be captured using a digital camera. The AFM data are presented as false color images, with contour intervals (see legends to figures) selected according to the feature size.

Supporting scanning electron microscope (SEM) images were acquired using a Philips XL30 ESEM with Oxford Instruments energy dispersive X-ray analysis (EDAX) system.

Sample Preparation and Handling

The brass substrate discs (68% copper/32% zinc; diameter 3 cm; thickness 1 mm, from Nobles Engineering, Northamptonshire, U.K.) are supplied with a plastic film covering one side. Prior to preparation each disc was labeled, via etching on the exposed side. The plastic film was peeled off to reveal a virgin surface, which was washed in commercial detergent and rinsed with acetone to remove any residual matter. Initial imaging of sample 1 (see below) corresponds to a blank disc viewed at this stage. The discs were then polished to a mirror finish using household Brasso™, washed with commercial detergent, and rinsed with acetone. Later imaging of sample 1 (see below) corresponds to a blank disc viewed at this stage.

All fingerprints were provided by the same donor. Prior to deposition, the donor's hands were thoroughly washed and dried. The time allowed for sweat development was in the range 10–20 min at laboratory temperature (nominally 20°C); sample 2, prepared under cooler conditions, used additional sweat induction in a latex glove. After fingerprinting, the samples were treated to selected humidity and temperature conditions to explore image development effects, as summarized in Table 1. Sample 2 was subjected to elevated humidity environment at room temperature, by placement in a sealed vessel also containing a beaker of water; it was removed after 9 days, washed and imaged. Sample 3 was placed in a similar sealed humid environment, but after 4 days was removed and placed (in air) in an oven at 100°C for 4 h; it was then removed, washed at room temperature, and imaged. Sample 4 was also placed in a sealed humid environment, but for a period of 8 days,

TABLE 1—*Summary of sample preparation procedures and conditions.*

Sample	Surface Preparation	Sweat Development	Sweat Type	Sample Treatment
1	As received	None	None	Imaged as delivered; polished and re-examined
2	Polished	20 min total, including 10 min inside glove	Eccrine	9 days in sealed container at room temperature/100% relative humidity
3	Polished	20 min, palms rubbed before deposit	Eccrine	4 days in sealed container at room temperature/100% relative humidity, followed by 3 h in air at 100°C
4	Polished	20 min, palms rubbed before deposit	Eccrine	8 days in sealed container at room temperature/100% relative humidity, followed by exposure to Bunsen burner flame for 75 sec
5	Polished	30 min	Eccrine	Sealed container at 50°C/100% relative humidity, periodically removed for imaging

then removed and held in a Bunsen burner flame for 75 sec; after cooling, it was washed with detergent, rinsed with acetone, and imaged. After washing, each sample was protected from contamination by plastic film and storage in a sealed container. Sample 5 was placed in a sealed vessel also containing a beaker of water and placed in an oven at 50°C. As described below, this sample was briefly removed at intervals for imaging, then replaced in the elevated humidity/elevated temperature environment to allow continued development.

Results and Discussion

In this section we define the problem and select the parameters for exploration. Figure 1 shows a photograph of a typical fingerprint deposited on a brass substrate. For visual comparison (to complement the AFM data shown below) of the influence of substrate surface finish, 50% of the surface was polished and 50% left as received (unpolished). Ridge features associated with the deposit of eccrine sweat transferred upon contact between the finger and sample are clearly visible, although fine detail is not at this resolution.

FIG. 1—*Photograph of a typical fingerprint on a brass substrate. Prior to deposition of the fingerprint, the left hand side of the substrate was polished (see main text for details); the surface finish of the right hand side is as received.*

There are also clear differences in visibility of the ridges on the two surfaces, a distinction upon which we will focus. Simplistically, the experimental strategy is to use the AFM to obtain a high resolution image of (selected regions of) this surface. The high spatial resolution of the AFM makes it sensitive not only to the fine detail we wish to study but also to the imperfections (e.g., manufacturing and handling marks) on the metal surface. The problem is that the transferred material is not deposited on a perfectly smooth surface; consequently, any raised or depressed features (deposits or etched areas) will not be viewed as deviations from a perfectly smooth surface.

The scope of the problem is demonstrated by Fig. 2, which shows an AFM image of what might (or might not, at this stage of the argument) be a feature resulting from a section of ridge detail deposited on one of the brass discs as received (sample 1, prior to polishing). The main feature is *c.* 30 μm wide and *c.* 600–800 nm deep (varying along its length). However, there are also a number of features on the order of 10 μm wide and 100–200 nm deep, which are present both on the unetched exterior surface and on the interior surfaces of the putative etch groove. From the perspective of a fundamental study of the scale and rate of formation of fingerprint-generated etched images, the latter complicate the situation considerably and make any assignment uncertain. In the context of unequivocal recognition of ridge features for identification purposes, the outcome would be ambiguous.

As a more simplistic starting point we therefore examined polished (optically smooth) surfaces, prepared as described in the

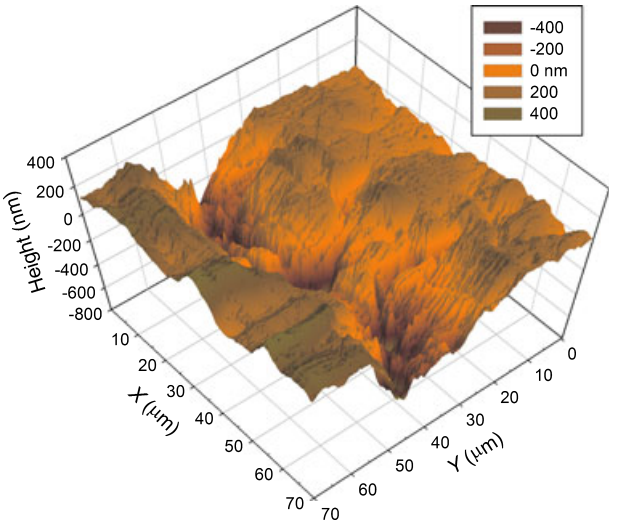

FIG. 2—*AFM image from the unpolished (as received) brass substrate, sample 1 (prepared as in Table 1). Note different horizontal and vertical scales and false color vertical representation, as indicated.*

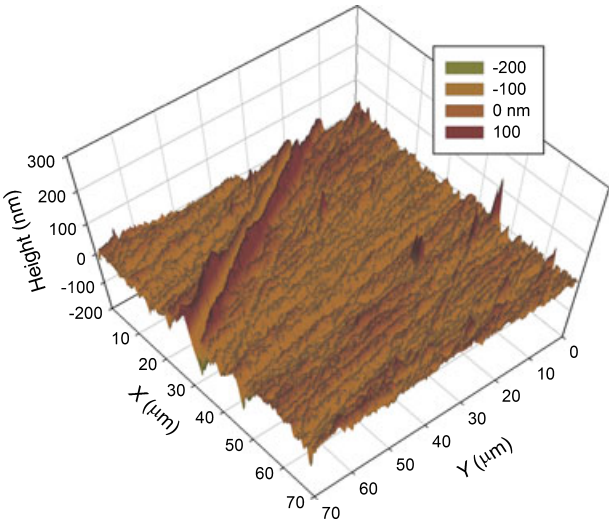

FIG. 3—*AFM image from the brass substrate, sample 1, after polishing (see Table 1).*

Materials and Methods section. While this is not realistic for the end application, it does allow unambiguous establishment of the methodology and definition of its capabilities and limitations. Figure 3 shows a typical AFM image of the same brass disc (sample 1) *after* polishing, from which two things are apparent. First, the mean surface roughness is decreased to features that are on the order of 1 µm wide and typically 20 nm deep. Second, where residual large machining features exist, they are obvious and unambiguously assignable. Specifically, the combination of characteristics exemplified by the linear scratch in Fig. 3 (approaching 5 µm wide and in excess of 100 nm deep) means that it could not be confused with the size or shape of the smaller polishing features or, as will be apparent later, fingerprint ridge detail.

The above observations mean that polished metal substrates provide surfaces on which ridge detail can be readily imaged not only at full-ridge resolution, but also at the higher resolution required for investigation of the ridge-deposit-to-etch feature transition that is at the heart of the imaging phenomenon. We now proceed to explore the effects of humidity and temperature, increases in both of which are generally perceived to accelerate corrosion processes, on the image generation.

Effect of Humidity on Image Development

In this section we consider the effect of elevated humidity but nonelevated (ambient) temperature. Figure 4 shows a representative example of ridge detail on a polished brass sample (sample 2) maintained at room temperature in a humid environment. Although the whole print image was somewhat patchy, exploration of the surface revealed a collection of similar ridges, along with ridge endings and other features typically associated with fingerprints. The eccrine sweat-derived deposit is clearly visible as a curved track *c.* 25 µm wide and 400 nm high. This feature is approximately a factor of 4–5 larger (in width and height) than the residual features on the polished substrate (see Fig. 3).

Interestingly, when the same procedure was employed with unpolished discs, similar features were visible but their outlines—and thus estimation of shape and dimension—were complicated by the slightly (but not dramatically) smaller machining imperfections on the surface. The common feature—most obviously on the smooth substrates but also on the rough substrates—was that all of

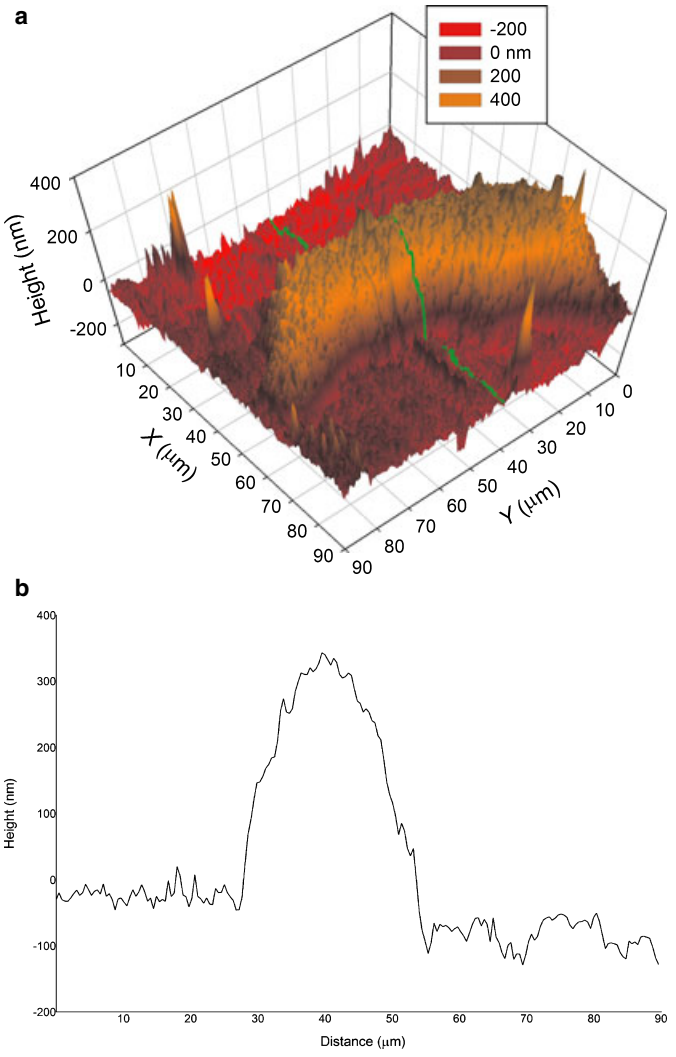

FIG. 4—*AFM images from the polished and printed brass sample 2 (see Table 1). (a) 3D image showing (part of) ridge detail. (b) 1D linescan across ridge detail, as indicated by green line across center of (a).*

these were *raised features*. We did not observe the *depressions* (trenches or pits) that would result if corrosion and subsequent metal loss from the surface had taken place. One possible inference is that on the timescales employed (which are realistic for many crime scene investigations) the conditions of elevated humidity preserve the sweat deposit by preventing complete evaporation of the volatile components, but the ambient temperature does not drive the corrosion reaction sufficiently rapidly to generate an etched image in the metal.

Prior experience (1,16–18) suggests that any residual sweat components would not survive the washing regime prior to imaging. We are therefore driven to consider the alternative inference that this adherent and durable deposit might be an oxide coating resulting from oxidation of the metal in a situation (a gas, rather than solution, environment) where it is unable to leave the surface. In support of this hypothesis, we (1,18) and others (16,17) have demonstrated previously that exposure to ambient temperature and humidity for a few days results in sufficient corrosion of these metal substrates for it to be visible to the naked eye (as a tarnished appearance) after the washing regime used here, which is sufficient to remove the initial sweat deposit. Clarification of this issue via chemical speciation is an important goal for subsequent study.

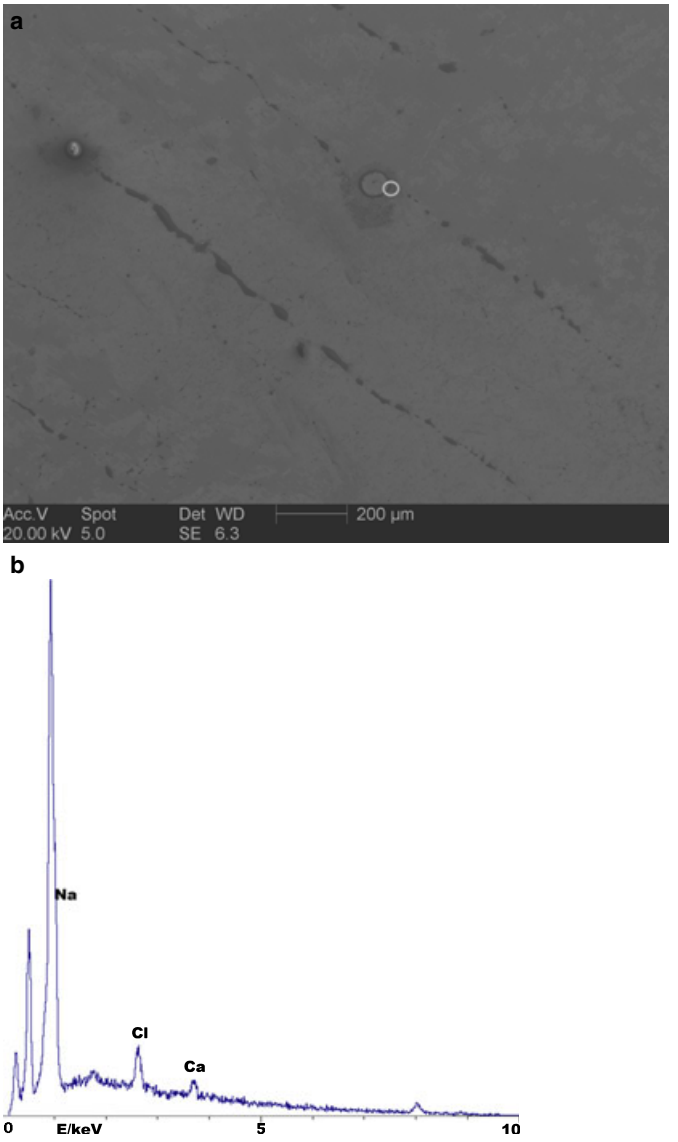

FIG. 5—*(a) SEM image of sample 2, showing multiple ridges, one of which was imaged in part in Fig. 4. (b) EDAX elemental scan of the part of sample 2 represented by the circled region in (a). Beam energy set to 10 keV to remove contributions of copper and zinc (from the brass substrate). Annotations indicate elemental assignment of peaks.*

Some pertinent information is provided by the supporting evidence of a lower resolution image showing multiple ridges. Figure 5*a* shows an SEM image of a larger part of the print of Fig. 4. Four ridges are clearly visible (running from top left to bottom right of the figure), as are two pores (one of which is circled in the image). Comparison of the images and differing lateral scales of Figs. 4 and 5*a* show that the feature in Fig. 4 assigned to a ridge is indeed of the correct size. This comparison also shows the dramatic enhancement in image quality and detail accessible with the AFM, an attribute that we will exploit further.

The observation that corrosion leading to pit/trench formation has not occurred demands an answer to the question as to whether this is because the required chemical agents were not present or whether the energetics of the system were inadequate. In chemical terms, the rate of a reaction is given by the product of concentration(s) and a temperature-dependent rate constant: the question is which of these is the limiting factor. This distinction is made by the EDAX spectrum of Fig. 5*b*, which relates to a spot located as

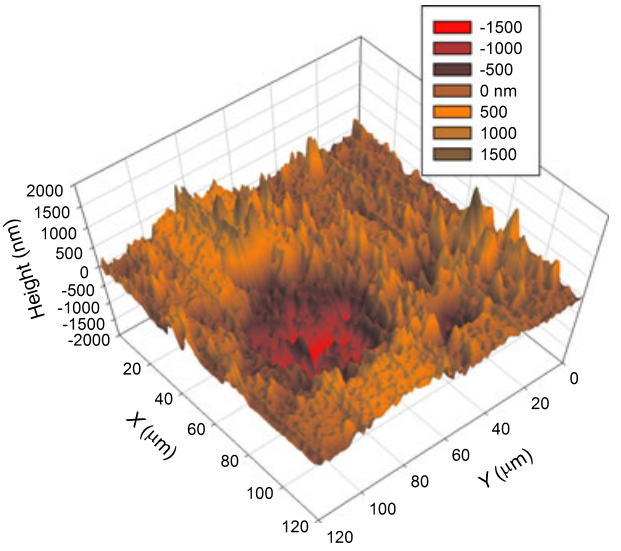

FIG. 6—*AFM image from the polished and printed brass sample 3, after heat treatment in air at 100°C.*

indicated by the white circle on the image of Fig. 5*a*. There is unequivocal evidence to indicate the presence of sodium and chloride ions, i.e., the constituents of salt, as well as lower levels of calcium secreted in the sweat. It is thus clear that all the required chemical species are present for corrosion. The conclusion is therefore that the reason for the lack of corrosion is insufficient energy to activate a kinetically rather slow reaction. We therefore now explore the effect of increased temperature as a source of energy.

Effect of Temperature on Image Development

Since elevated humidity alone did not generate etched images in the metal substrate, the effect of additional enhancement by increased temperature was explored. Figure 6 shows an AFM image of a region of a polished brass sample (sample 3) subjected to moderate heat (100°C in air) after storage in a humid environment. On this sample, a number of trenches or pits were seen, with width varying from 50 to 80 µm and depth 2 µm, and there were significantly fewer deposits of the sort found in the nonheat-treated samples (see previous section, Figs. 4 and 5). A lower resolution photographic image of sample 5 (from the time lapse observations discussed in detail below) is shown in Fig. 7.

The scale of the features in Fig. 6 is clearly incompatible with fine polishing marks (see Fig. 3). Their shape and, to a lesser extent, their scale are also clearly incompatible with the few residual machining marks not removed by polishing (see the very regular linear scratch in Fig. 3). Finally, the fact that rather moderate heat treatment changes the surface features is incompatible with the brass substrate alone. We are therefore driven to the conclusion that the combination of elevated humidity and heat has generated the observed features derived from ridge deposits. However, the extent of image development is rather limited and by eye the print appears rather dotted. Pragmatically, the sample falls between two useful extremes: the heat treatment has driven off sufficient volatile material from the initial deposit to make conventional observation uncertain but it has not sufficiently developed the pits and trenches to make the corrosion-based image clear.

A more extreme form of heat treatment, exposure to an open Bunsen burner flame (*c.* 300°C for 75 sec; sample 4), generated images of the type illustrated in Fig. 8. This sample showed only

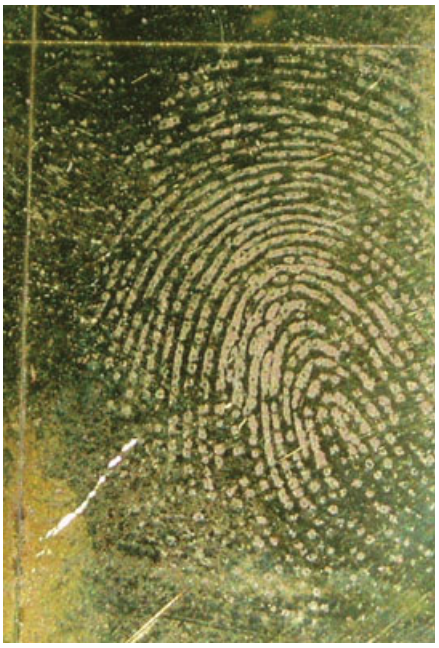

FIG. 7—*Photograph of whole fingerprint for sample 5. The horizontal and vertical lines are registration marks used to locate the AFM tip for repetitive examination of the same area of the surface (as in Fig. 10).*

small residual amounts of deposited material and had pronounced pits. In the image shown, one can see a small raised area adjacent to the pit. The diameter of the pit is 50 μm and the depth *c.* 2 μm, as for the 100°C treated sample, but the pit definition is much sharper.

Another image from the same sample is shown in Fig. 9. This is a particularly well-defined example of a trench, which we propose is the result of local corrosion beneath a section of ridge deposit. The flat baseline, representing the pristine polished substrate, can be seen to either side of the trench. The characteristic dimensions associated with the trench of Fig. 9 and the pit of Fig. 8 (which are commensurate with the dimensions of fingerprint ridge detail) mean that they cannot be confused with the substrate polishing marks or residual machining marks of the bare substrate in Fig. 3.

Image Development

The features seen in Figs. 4 and 9 (and replicate observations) essentially represent the start and end of the image development process. It is clear that enhancement by humidity *and* temperature elevation are required, but images of the sample of Fig. 9 give no indication of whether the forcing conditions employed are barely adequate or far in excess of what is required to generate the image. With a view to practical application of the method, there is considerable interest in understanding the temporal evolution of the etched image. For cases involving objects in a fire, this would be relevant to decisions about searching for items upon which images might be expected to be developed (1). For cases of objects not subject to heat but upon which there might be latent fingerprints that could be deliberately developed by application of humidity and heat, this would be critical to optimization of conditions for developing the image. Finally, it would be relevant for discarded objects at scenes not identified until some time after the crime.

We therefore attempted to observe the development of a section of ridge detail by time lapse imaging of the sample. Figure 10 shows a sequence of images of the same area of a brass surface (sample 5) on which one can see a section of a ridge deposit. This sample was exposed to a humid environment (saturated water vapor) at moderately elevated temperature (50°C, to give a convenient rate of change) and removed at periodic intervals for observation. Feature locations were reproducibly identified by the placement of a scratched cross-hair on the surface (as seen in the registration marks on the low resolution photograph in Fig. 7), some distance from the area investigated; the positioning system of the AFM allowed sample translation to repeatedly observe the same area. In the image shown in Fig. 10, the primary feature is a deposit (corresponding to a ridge) that progressively decreases in height and flattens on a timescale of days. One can also see the presence of a depression surrounding the deposit. While not at this stage proof, this and similar images suggest that the formation of etch trenches and pits does not initially take place *beneath* the ridge

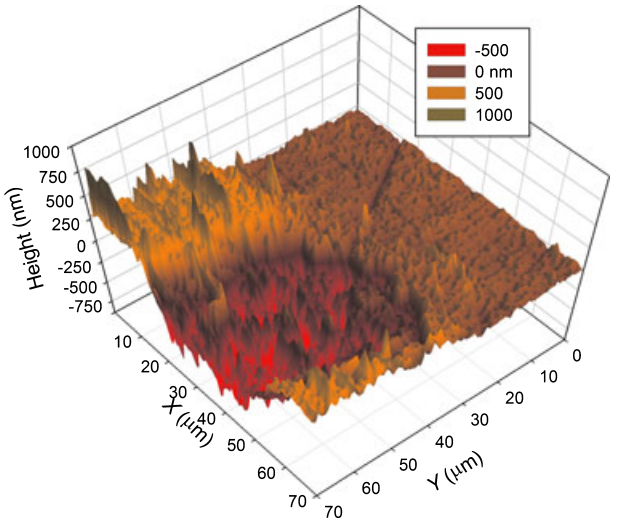

FIG. 8—*AFM image from a part of the polished and printed brass sample 4 (after heat treatment in a Bunsen burner flame) showing a pit (at front corner of image) created by corrosion of the surface.*

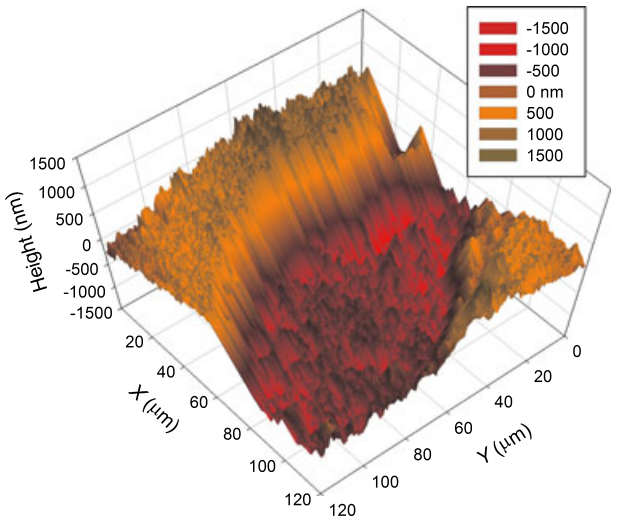

FIG. 9—*AFM image from a part of the polished and printed brass sample 4 (after heat treatment in a Bunsen burner flame) showing a trench created by corrosion of the surface.*

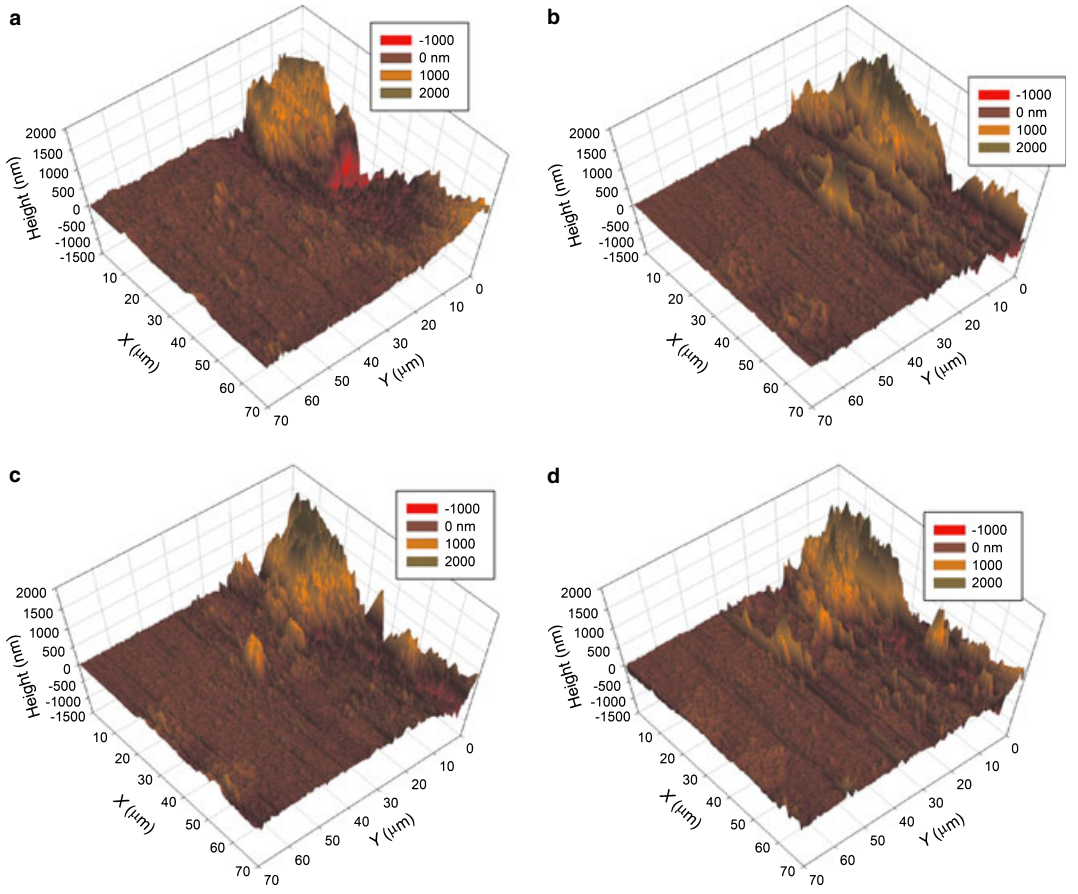

FIG. 10—*AFM images from the polished and printed brass sample 5. The images are of the same region, identified by calibrated horizontal (x,y) translation of the AFM tip from registration lines of the type shown in Fig. 7. Time elapsed from fingerprint deposition and placement into a humid environment at 50°C (see Table 1): a: 4 days; b: 7 days; c: 8 days; d: 11 days.*

deposits, but rather *around* them. A chemical explanation for this would be that corrosion requires water, salt, *and* oxygen to be available, and that all these agents are only present at the metal/deposit/air three-phase boundary. Beneath the deposit there is insufficient oxygen to drive corrosion and beyond the deposit the availability of water/salt is minimal. Pursuit of this hypothesis will be the subject of future study.

Given the unprecedented level of detail seen in the images above, it is interesting to ask how much of the exceptional spatial resolution of the AFM can be exploited in this context. Figure 11 shows an AFM image of a region not dominated by ridge detail. There are a number of small deposits, best described as depressed hemispheres typically 5–10 µm in diameter and 0.5–1 µm in height; note that the deliberately selected different lateral and vertical length scales in the AFM image alter the superficial visual perception. Comparison of the line scans (not shown) that in one case intercept and in another case avoid these features show that they can be clearly resolved on the comparatively flat polished brass surface. These features are not representative of generally acknowledged fingerprint features. However, their presence after—but absence before—placement of the fingerprint on the surface signals that they represent transfer of material from finger to metal. We attribute them to small-scale spatter associated with the delivery of the fingerprint onto the surface. One might reasonably anticipate that they would be capable of generating smaller scale corrosion pits on the surface, whose presence would complicate image analysis in much the same way that was true of surface roughness present on the unpolished metal surfaces. Given their association with the formation of the fingerprint, there is no obvious way to avoid the presence of these small features; ultimately they may limit image interpretation.

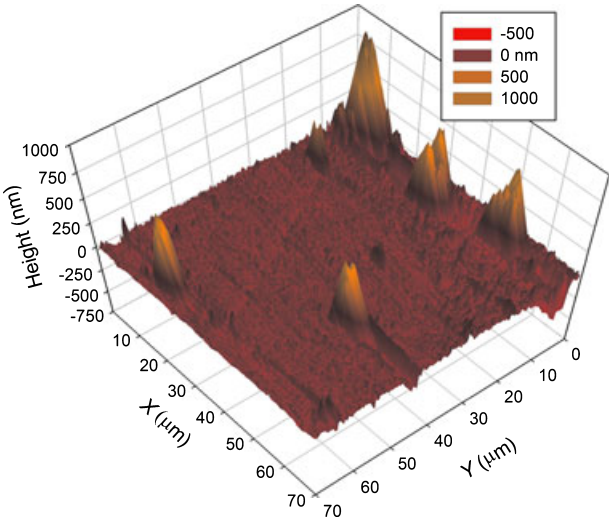

FIG. 11—*AFM image from polished and printed brass sample 5 after 2 days in a humid environment at 50°C (see Table 1). The area shown is one not containing ridge detail, complementary to Fig. 10.*

Conclusions

The AFM is capable of imaging fingerprint ridges at an unprecedented level of detail. Individual features—ridges, ridge endings, pores—and their fine structure are directly observable via topographical images of the material transferred from finger to (brass) substrate. On a typical machined brass surface, the feature size of the ridges (tens of micrometers) is slightly larger than that of machining marks (*c.* 10 μm), such that the ridges are visible but determination of their detailed shape and characterization are not trivial. On polished surfaces, where the substrate feature size is decreased to *c.* 1 μm, visualization of the ridge detail is significantly enhanced. Elemental analysis (using EDAX, coupled with SEM imaging) at a lateral spatial resolution comparable with the width of the ridges shows the presence of sodium and chlorine species, i.e., the constituents of salt.

Leaving the sample at ambient temperature at high humidity does not change the image appreciably. It is likely that there is some evaporative loss of volatile components of the sweat deposit and some gain of surface material through oxidation (tarnishing) of the metal, but functionally the appearance of the ridge detail does not change significantly. Mild heating (at 100°C) in air almost certainly increases the rates of both these processes, but does not change the topographical image greatly. In sharp contrast, brief heating of the sample in a flame (typical temperature 300°C) dramatically changes the image: instead of raised features representing the deposited ridge detail, one observes a series of depressions. These pits and trenches are believed to result from the (thermally enhanced) corrosion process between what is effectively a salt solution and the brass. This process is sufficiently localized that it has the potential to generate a negative topographical image of the fingerprint.

AFM examination of surface regions *between* ridges revealed small, approximately circular, deposits that were not present on the unprinted substrates. These are most likely either microscopic "spatter" of sweat components or are associated with transfer of particulates from the finger. When they are clearly between ridges, these do not interfere with the surface analysis. However, if their surface population were to be very high and their locations were adjacent to the ridges, it is possible that they might limit the level of analysis of ridge detail using the present methodology.

Having demonstrated here the concept, the details of the corrosion process are a topic for future study. However, we speculate that if the requirement is the presence of water and salt (from the ridge deposit) *and* oxygen (from the ambient atmosphere) this would lead to the process initially taking place at the three-phase boundary between the metal, deposit, and air, i.e., along the periphery of the ridges. The AFM is capable of following the temporal evolution of this process, which will prove to be important for the optimization of conditions for generation of a faithful and durable image of the initial fingerprint deposit.

Acknowledgments

We thank Mr. Graham Clark of the Engineering Department at the University of Leicester for help with acquisition of SEM images and Dr. Karl Ryder of the Chemistry Department at the University of Leicester for helpful discussion of AFM images.

References

1. Bond JW. Visualization of latent fingerprint corrosion of metallic surfaces. J Forensic Sci 2008;53:812–22.
2. Markovic NM, Ross PN. Surface science studies of model fuel cell electrocatalysts. Surf Sci Rep 2002;45:117–129.
3. Anariba F, DuVall SH, McCreery RL. Mono- and multilayer formation by diazonium reduction on carbon surfaces monitored with atomic force microscopy "scratching." Anal Chem 2003;75:3837–44.
4. Naumann R, Schiller SM, Giess F, Grohe B, Hartman KB, Karcher I, et al. Tethered lipid bilayers on ultraflat gold surfaces. Langmuir 2003;19:5435–43.
5. Lipkowski J, Ross PN, editors. Imaging of surfaces and interfaces. New York, NY: Wiley-VCH, 1999.
6. DiNardo NJ. Nanoscale characterization of surfaces and interfaces. New York, NY: VCH, 1994.
7. Macpherson JV. Electrochemical AFM. In: Bard AJ, Stratmann M, Unwin PR, editors. Encyclopedia of electrochemistry. Vol. 3. Weinheim: Wiley-VCH, 2003;415–43.
8. Pascoe MW, Richardson MOW. A new method for the detection of thin films on steel. Wear 1971;18:76–8.
9. Czekanski P, Fasola M, Allison J. A mechanistic model for the superglue fuming of latent fingerprints. J Forensic Sci 2006;51:1323–8.
10. Bowman V, editor. Manual of fingerprint development techniques, 2nd rev. edn. Sandridge, UK: Police Scientific Development Branch, Home Office, 2004.
11. Bandey H, Kent T. Superglue treatment of crime scenes. Sandridge, UK: Police Scientific Development Branch, Home Office, 2003, Report No.:30/03.
12. Bersellini C, Garofano L, Giannetto M, Lusardi F, Mori G. Development of latent fingerprints on metallic surfaces using electropolymerization processes. J Forensic Sci 2001;46:871–7.
13. Cantu AA, Leben DA, Ramotowski R, Kopera J, Simms JR. Use of acidified hydrogen peroxide to remove excess gun blue-treated cartridge cases and to develop latent prints on untreated cartridge cases. J Forensic Sci 1998;43:294–8.
14. Smith K, Kauffman C. Enhancement of latent prints on metal surfaces. J Forensic Ident 2001;51:9–15.
15. Migron Y, Mandler D. Development of latent fingerprints on unfired cartridges by palladium deposition: a surface study. J Forensic Sci 1997;42:986–92.
16. Williams G, McMurray HN, Worsley DA. Latent fingerprint detection using a scanning Kelvin microprobe. J Forensic Sci 2001;46:1085–92.
17. Williams G, McMurray N. Latent fingermark visualization using a scanning Kelvin probe. Forensic Sci Int 2007;167:102–9.
18. Bond JW. The thermodynamics of latent fingerprint corrosion of metal elements and alloys. J Forensic Sci 2008;53:1344–52.
19. Bond JW. On the electrical characteristics of latent finger mark corrosion of brass. J Phys D Appl Phys 2008;41(12):125502.
20. Bar-Lev A. Semiconductors and electronic devices. Hemel Hempstead: Prentice Hall, 1993;96–124.
21. Sze SM. Semiconductor devices. Danvers: Wiley, 2002;224–53.
22. Fraser DA. The physics of semiconductor devices. New York, NY: Oxford University Press, 1986;132–63.
23. Kolb DM. Electrochemical surface science. Angew Chem Int Ed 2001;40:1162–81.
24. Moffatt TP. Electrochemical STM. In: Bard AJ, Stratmann M, Unwin PR, editors. Encyclopedia of electrochemistry. Vol. 3. Weinheim: Wiley-VCH, 2003;393–414.
25. Zhang JD, Demetriou A, Welinder AC, Albrecht T, Nichols RJ, Ulstrup J. Potential-induced structural transitions of DL-homocysteine monolayers on Au(111) electrode surfaces. Chem Phys 2005;319:210–21.

Additional information and reprint requests:
A. Robert Hillman, D. Phil.
Department of Chemistry
University Road
University of Leicester
Leicester LE1 7RH
U.K.
E-mail: arh7@le.ac.uk